A Novel Design of a Low-loss and Low-cost Ku-Band Bandpass Filter for VSAT Applications

Mai Van TA, Kieu Khac PHUONG, Nguyen Duc TRONG, Nguyen Thuy LINH, Tran Thi Thu HUONG, Nguyen Tuan HUNG, Luong Duy MANH

Faculty of Radio-Electronics, Le Quy Don Technical University, 236 Hoang Quoc Viet, Co Nhue, Bac Tu Liem, Hanoi, Vietnam

tamv@lqdtu.edu.vn

Submitted February 18, 2025 / Accepted June 3, 2025 / Online first July 2, 2025

Abstract. *This paper proposes a novel method to design low-loss and low-cost Ku-band bandpass filters for VSAT applications based on substrate-integrated-waveguide technology. Narrow bandpass filters employed high-order resonant mode TE_{301} exhibited high selectivity. However, its bandwidth is not enough for VSAT applications. In this paper, we proposed a method to widen the bandwidth of narrow-band filters to meet the bandwidth requirement of VSAT applications. This approach maintains high selectivity while still achieves low insertion loss. The proposed filter was fabricated using a low-cost material. Measurement shows a good agreement with simulated results. Mid-band measured insertion loss and return loss were 1.8 dB and 19.4 dB, respectively. Such low losses were obtained owing to taking advantage of a high-quality factor of high-order mode TE_{301} of oversized rectangular cavities.*

Keywords

High/low order mode coupling, substrate integrated waveguide, fractional bandwidth (FBW)

1. Introduction

Metallic waveguides are a good technology at high-frequency bands such as X-band and Ku-band owing to high power handling capacity and low loss. However, such bulky waveguides are not suitable for circuit integration. For that purpose, microstrip technology is advantageous. Indeed, microstrip circuits are dominant in low-frequency microwave bands such as the L-band. However, as frequency increases, microstrip circuits suffer high losses. Substrate integrated waveguide technology has emerged as a promising technology for microwave devices, especially at high frequency such as X-band and Ku-band [1–5]. This originates from lower loss compared to traditional microstrip technology. Two metallic via lines act as traditional metallic waveguide walls for confining waves, mitigating wave leakage for loss improvement. Various SIW bandpass filter types were proposed such as complementary split-ring resonator (CSRR) [6], [7], inductive post [8], [9], and rectangular-cavity-based filters [10–15]. CSRR filters are compact owing to evanescent-wave transmission. Inductive post filters are simple in construction. However, the selectivity of CSRR and inductive post filters is relatively low. This is because moderate quality factors of CSRR and inductive post limit the selectivity of such filters.

For rectangular-cavity-based filters, the selectivity can be improved by cascading multiple resonant cavities [16]. However, this led to increased in-band insertion loss (IL) and larger filter size. Alternatively, the high/low order mode coupling technique creates coupling paths between the source and load, thus generating transmission zeros (TZs) on both sides of the passband, thereby improving the filter's selectivity [17], [18]. Moreover, for a multimode SIW cavity, higher-order modes yield higher unloaded quality factors than that of lower-order ones [18]. The use of high-order modes such as TE_{201} and TE_{301} could result in both high selectivity and low IL [18], [19].

An X-band narrow bandpass filter reported in [18] employed two TE_{301}-mode resonant cavities to create the passband and a TZ below it. Furthermore, it employed an additional TE_{101}-mode cavity to create another coupling path between the two TE_{301} cavities, thus generating another TZ above the passband. This filter exhibits a high selectivity on both sides of the passband. Nevertheless, this filter has a narrow FBW of 1.1%. This value of FBW does not meet the bandwidth requirement for VSAT applications, which is typically about 5% to 6%.

In this paper, we propose a novel method to design a Ku-band filter for VSAT applications. For this, we present another coupling path between the two TE_{301} cavities to widen the bandwidth of the filter reported in [18]. This allows to achieve a low IL thanks to the high-quality factor of TE_{301} cavities, while still retaining the high selectivity. Owing to the high-order mode, the quality factor of cavities was kept high even when the filter was fabricated using a low-cost substrate PTFE. Measured results agreed well with simulations.

DOI: 10.13164/re.2025.0445

The rest of the paper is organized as follows. Section 2 presents the filter design and operation principle. The results are discussed in Sec. 3. Finally, the conclusion of the paper is given in Sec. 4.

2. Design and Analysis

Ku-band BPFs used for VSAT satellite communication systems require a wide FBW of approximately 5%–6%, along with low IL and high selectivity. The filter reported in [18], which operates in X-band, exhibited a high selectivity. Moreover, employing a high-order mode results in a compact size. However, its FBW was just 1.1%. This paper proposes a method to widen the bandwidth of the filter structure reported in [18] to design Ku-band BPFs used for VSAT applications. This allows to achieve low IL owing to the high-quality factor while still maintaining the high selectivity.

The building block of the designed filter is a singlet. A singlet is a first-order BPF structure. It consists of a resonant cavity that can generate a TZ either below or above the passband using a coupling path between the source and load. Figure 1 shows a rectangular SIW cavity acting as a singlet.

A SIW-based singlet is essentially a rectangular SIW cavity with different high/low order propagating modes. Here, *W* and *L* are the width and length of the rectangular SIW cavity, respectively. *d* is the diameter of the vias; *p* is the spacing between two vias. Two 50 Ω microstrip lines with a width of W_m are used as feeding lines. Coupling gaps W_f are used to couple the cavity with the source and load.

The condition for the electromagnetic field inside the SIW cavity not to be radiated out through the slots between the vias is given by [20]:

$$d < 0.2W,\ d < p < 2d. \tag{1}$$

The effective width and length of the rectangular SIW cavity are calculated using the following formulas [20]:

$$W_{\text{eff}} = W - \frac{d^2}{0.95p}, \tag{2}$$

$$L_{\text{eff}} = L - \frac{d^2}{0.95p}. \tag{3}$$

The resonant frequency of the modes in the rectangular SIW cavity is determined as [20]:

$$f_{\text{TE}_{m0q}} = \frac{c}{2\sqrt{\varepsilon_r}}\sqrt{\left(\frac{m}{W_{\text{eff}}}\right)^2 + \left(\frac{q}{L_{\text{eff}}}\right)^2} \tag{4}$$

where m, $q = 1, 2, 3, \ldots$; $c = 3 \times 10^8$ m/s is the speed of light; ε_r is the relative permittivity of the substrate.

Figure 2 illustrates the electric field distribution of different modes inside a rectangular SIW cavity.

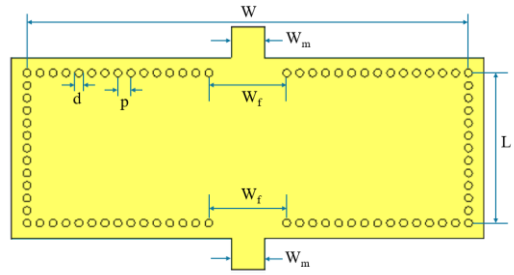

Fig. 1. A rectangular SIW cavity resonator acting as a singlet.

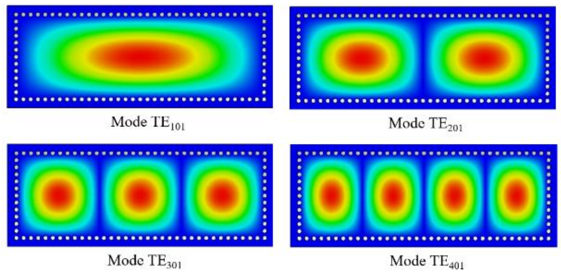

Fig. 2. Electric field distribution of different modes in the rectangular SIW cavity resonator.

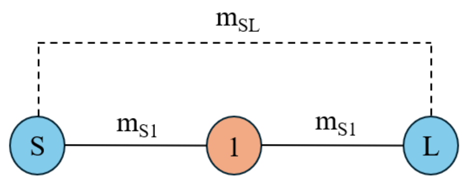

Fig. 3. Coupling diagram of a singlet.

This singlet structure utilizes different propagating modes to create separate energy transmission paths from the source to the load, thereby generating the necessary TZs both below and above the passband [17]. The coupling scheme of a singlet is shown in Fig. 3. Here *S*, *L* and *1* are the source, load, and resonant cavity, respectively. m_{S1} and m_{SL} are the direct coupling coefficient between the cavity and the source/load and the coupling coefficient between the source and load, respectively.

The normalized frequency of the TZ is calculated as [21]:

$$\Omega_{\text{TZ}} = \frac{m_{S1}^2}{m_{SL}}. \tag{5}$$

Thus, the position of the TZ depends on the sign of the source-load coupling coefficient m_{SL}. If $m_{SL} < 0$, the TZ is located below the passband; conversely, if $m_{SL} > 0$, the TZ is located above the passband.

To obtain a Ku-band BPF with a wide passband, high selectivity, and low in-band IL, we propose a filter structure consisting of four coupled resonant cavities. Figure 4 depicts the structure of the proposed filter, and Figure 5 shows its coupling scheme. Resonant cavities R_1 and R_2 support the TE_{301} mode at the center frequency of the passband, which is 13.34 GHz, while resonant cavities R_3 and R_4 support the TE_{101} mode, also at 13.34 GHz. The TE_{101}

spurious mode in R_1 and R_2 at 12.6 GHz does not contribute to creating the passband but helps generate a TZ because the signal from the source to the load through cavities R_1 and R_2 via two different paths created by the TE_{301} and TE_{101} modes will produce a TZ below the passband.

The coupling gap g_1 between the two resonant cavities R_1 and R_2 is placed symmetrically at $W/2$, at this position the field of the even modes TE_{201} and TE_{401} is zero, thus eliminating the coupling effect of these modes on the lower and upper stopbands, thereby ensuring wide lower and upper stopbands. The two resonant cavities R_3 and R_4 are identical and through the coupling gaps g_2 will create additional signal coupling paths between R_1 and R_2, generating a TZ above the passband.

To clearly demonstrate the ability to widen the bandwidth of the proposed filter, we compare the passband of the proposed filter, which is shown in Fig. 4, and that of the filter without the R_4 cavity. The comparison is plotted in Fig. 7 of the next section. The structure of the filter without the R_4 cavity is shown in Fig. 6.

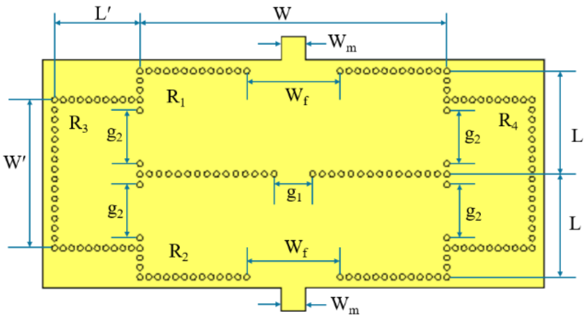

Fig. 4. Structure of the proposed BPF.

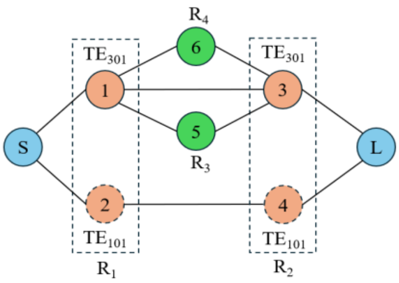

Fig. 5. Coupling diagram of the proposed BPF.

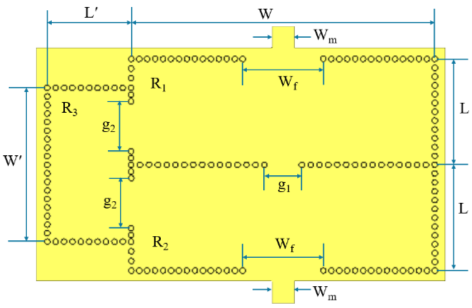

Fig. 6. Structure of the BPF filter without R_4 cavity.

The filter in this study uses a PTFE substrate with a dielectric thickness of 0.762 mm, a loss tangent of 0.0018, and a relative permittivity $\varepsilon_r = 2.55$. These parameters are given at 10 GHz by the substrate provider. Taking into account the frequency dependencies of material parameters, the "Const-fit. - automatic" fitting model in CST 3D electromagnetic simulator was selected for accurate simulation purposes. The via diameter and spacing between vias are chosen as $d = 0.5$ mm and $p = 0.8$ mm, respectively. The dimensions of the filter cavities are calculated for a center frequency of 13.34 GHz using (2), (3), and (4).

3. Results and Discussions

The CST 3D electromagnetic simulation software was used to simulate the different modes inside the rectangular cavity and the proposed filter's S-parameters. A relatively high calculated unloaded quality factor of 388 was obtained, which corresponds to the TE_{301} resonant mode of the rectangular cavity.

Figure 7 shows the frequency dependence of S_{21} for the filter with cavity R_4, which is indeed the proposed filter, and the filter without cavity R_4. Adding resonant cavity R_4 allows to widen the passband of the filter. This can be explained by that adding cavity R_4 introduces an additional energy coupling path for the signal between resonant cavities R_1 and R_2, resulting in more frequency components that can travel from the source to the load. Figure 10 also clearly shows that when the bandwidth of the filter is widened, a high selectivity is still maintained despite slight degradation. The TZ below the passband only reaches nearly –30 dB, which is because the position of this TZ is still slightly far from the center frequency of the passband, which is the frequency of the TE_{301} mode. To improve this TZ, it needs to be moved closer to the center frequency. The position of this TZ depends on the frequency of the TE_{101} mode. Therefore, the frequency of the TE_{101} mode needs to be brought closer to the frequency of the TE_{301} mode by reducing the W/L ratio of the resonant cavities R_1 and R_2 [18]. This is quite challenging because while changing the W/L ratio, calculations must be performed to ensure that the frequency of the TE_{301} mode remains at 13.34 GHz. The optimization will be carried out and reported elsewhere.

Figure 8 illustrates the dependence of S_{21} on the coupling gap g_1. It is obvious that changing the coupling gap g_1 will affect the coupling coefficient between the two resonant cavities R_1 and R_2, thus significantly affecting the position of the TZ in the upper passband. Changing g_1, however, has just a slight effect on the filter's passband.

Figure 9 illustrates the variation of S_{21} and S_{11} with the change of the coupling gap g_2. It is observed that increasing the coupling gap g_2 widens the passband. Furthermore, changing g_2 also alters the coupling coefficient between resonant cavities R_1 and R_2 through R_3 and R_4,

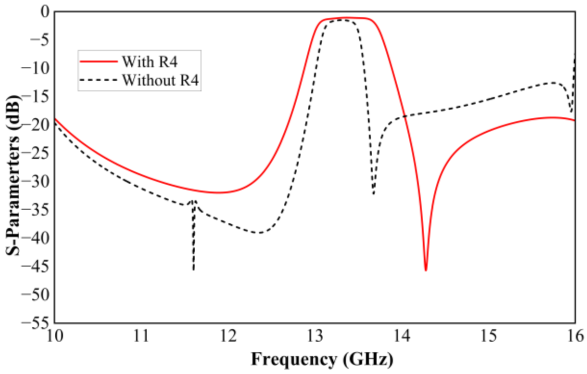

Fig. 7. Comparison of S21 between filters with and without R_4 cavity.

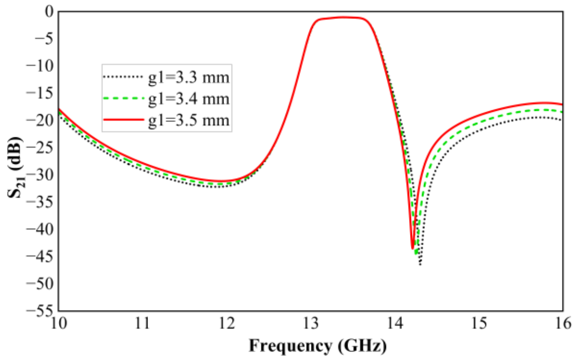

Fig. 8. Frequency dependence of S_{21} with various coupling gap g_1.

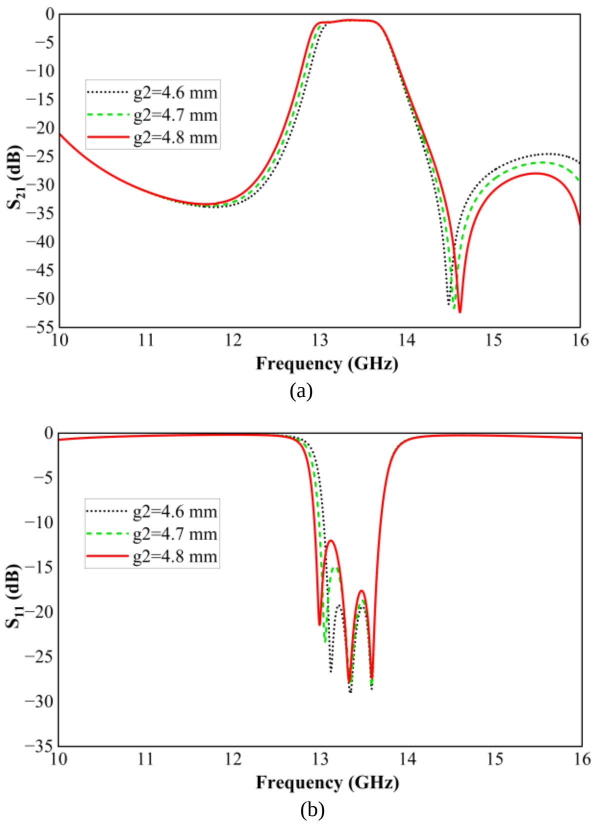

Fig. 9. Frequency response of S_{21} (a) and S_{11} (b) with varying coupling gap g_2.

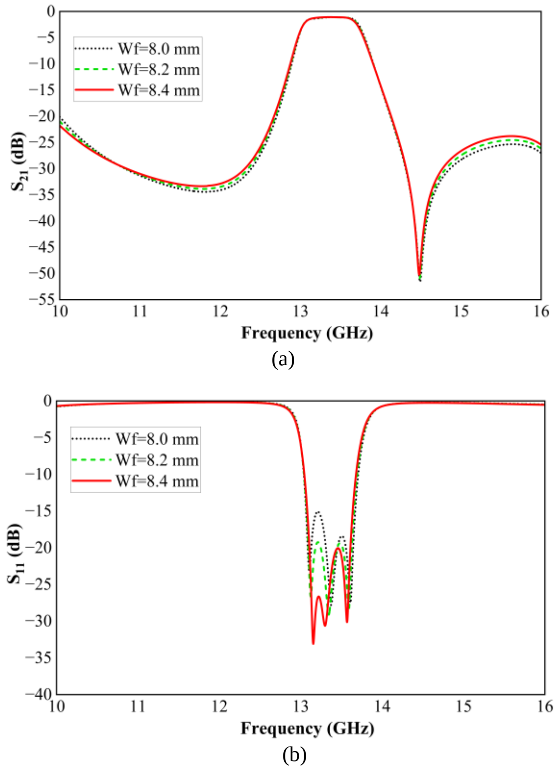

Fig. 10. Frequency response of S_{21} (a) and S_{11} (b) with varying coupling gap width W_f.

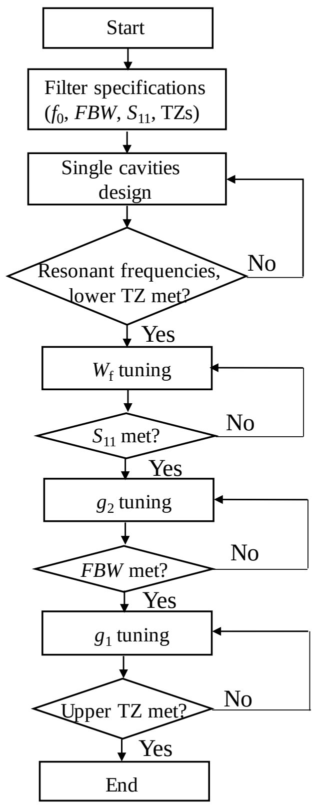

Fig. 11. Design flow of the proposed filter.

consequently affecting the position of the TZ above the passband. On the other hand, increasing g_2 adversely affects S_{11}, as observed in Fig. 9(b). However, this limitation can be overcome by adjusting the coupling gap W_f, as shown in Fig. 10(b).

Figure 10(a) shows the variation of S_{21} with the change in the coupling gap W_f. Changing the width of coupling slot W_f has a minimal effect on S_{21}. However, changing W_f will alter the coupling coefficients between R_1, R_2 resonant cavities and the source and load, thus mainly affecting S_{11}, as shown in Fig. 10(b). Therefore, we carefully adjust W_f to obtain a reasonable S_{11}.

In this work, coupling gaps g_1, g_2, and W_f are selected from investigations shown in Fig. 8, 9, and 10, respectively. The design flow of the proposed filter is summarized in Fig. 11. To experimentally validate the proposed structure, we fabricated a filter prototype using a low-cost PTFE substrate. Following the design flow, the dimensions of the fabricated filter are W = 28.4 mm, L = 9.7 mm, W' = 14.9 mm, L' = 7.9 mm, g_1 = 3.4 mm, g_2 = 4.6 mm, W_f = 8.2 mm, d = 0.5 mm, p = 0.8 mm, and W_m = 2.15 mm.

The measured results are shown in Fig. 13. There is a good agreement between the measured data and simulated results. A good measured mid-band IL of 1.8 dB was obtained. While the measured mid-band return loss (RL) was

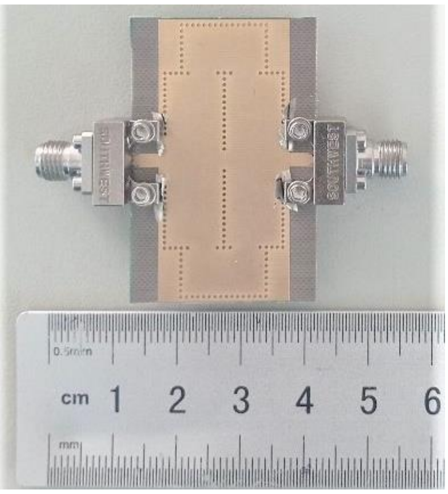

(a)

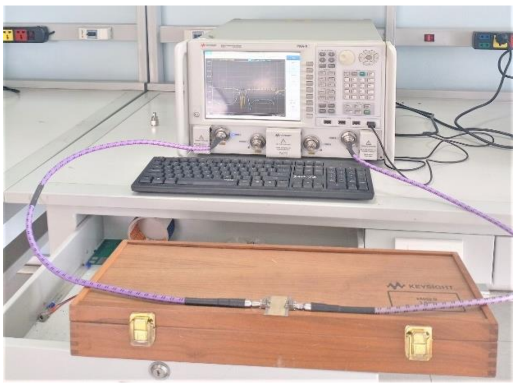
(b)

Fig. 12. Photograph of the fabricated filter (a) and measurement setup (b).

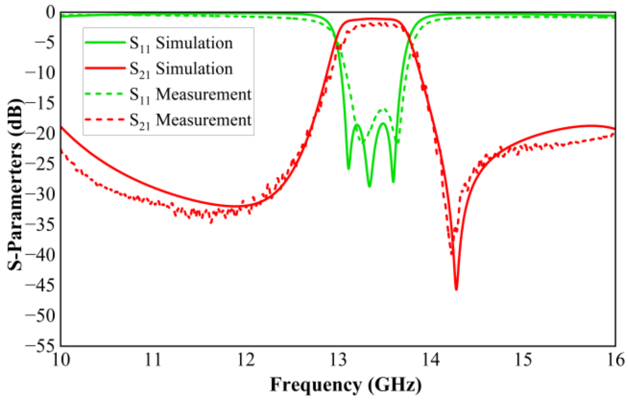

Fig. 13. Comparison of frequency responses between the simulated and measured filters.

19.4 dB. A slight deviation between the measurement and simulation is attributed to fabrication tolerance. The measured FBW of the fabricated filter was 5.8%. This can be effectively adjusted by tuning coupling gap g_2 as illustrated above in Fig. 9(a).

The photographs of the fabricated filter are given in Fig. 12(a). The measurement of the fabricated filter was performed using a vector network analyzer, N5242A from Keysight, as displayed in Fig. 12(b).

Table 1 shows a comparison of the parameters of the proposed filter with those of some BPFs based on SIW technology in some published works. The proposed filter exhibits a low mid-band IL while using a low-cost substrate. Moreover, it also exhibited a good mid-band RL.

4. Conclusions

This paper proposed a novel approach to design a Ku-band BPF for VSAT applications. We widened the passband for a narrow-band filter structure to meet the bandwidth requirement of VSAT applications by introducing an additional resonant cavity. The proposed filter operates in the Ku-band with a wide bandwidth of 775 MHz, which corresponds to FBW of 5.8%. The filter's bandwidth fully meets the requirements of VSAT satellite communication systems. A low mid-band IL of 1.8 dB was achieved by utilizing the high-quality factor of the high-order TE_{301} mode. The measured mid-band RL was 19.4 dB. At the same time, a high selectivity was ensured thanks to the TZs on both sides of the passband. The proposed filter has potential applications for Ku-band VSAT satellite communication systems.

Acknowledgments

This research is partly supported by Le Quy Don Technical University.

Ref.		[16]	[22]	[12]	[23]	[18]	This work
f_0 (GHz)		28.0	9.0	14.87	22.2	8.25	13.34
Mid-band IL (dB)		2.2	2.1	3.6	2.9	3.3	1.8
Mid-band RL (dB)		16.0	12.0	14.3	N/A	15.0	19.4
3dB FBW (%)		3.6	5.5	1.5	1.44	1.1	5.8
Size (λ_0^2)		0.8	0.67	2.1	0.8	1.8	1.76
Substrate		TLY-5	RT 5880	RT 5880	RO 5880	RT 5880	PTFE ZYF255DA
30 dB rejection start at	Lower ($f_0 - \Delta f_0$%)	2.4	6.5	2.3	3.3	1.9	7.9
	Upper ($f_0 + \Delta f_0$%)	5.7	6.7	2	3.8	1.2	5.9

Tab. 1. Comparison of the parameters of the proposed filter with the parameters of some SIW BPFs from previously published works.

References

[1] DESLANDES, D., WU, K. Single-substrate integration technique of planar circuits and waveguide filters. *IEEE Transactions on Microwave Theory and Techniques*, 2003, vol. 51, no. 2, p. 593–596. DOI: 10.1109/TMTT.2002.807820

[2] BOZZI, M., GEORGIADIS, A., WU, K. Review of substrate-integrated waveguide circuits and antennas. *IET Microwaves, Antennas and Propagation*, 2011, vol. 5, no. 8, p. 909–920. DOI: 10.1049/iet-map.2010.0463

[3] PRADHAN, N. C., KOZIEL, S., BARIK, R. K., et al. Bandwidth-controllable third-order bandpass filter using substrate-integrated full- and semi-circular cavities. *Sensors*, 2023, vol. 23, p. 1–15. DOI: 10.3390/s23136162

[4] CHENG, F., GU, C., ZHANG, B., et al. High isolation substrate integrated waveguide diplexer with flexible transmission zeros. *IEEE Microwave and Wireless Components Letters*, 2020, vol. 30, no. 11, p. 1029–1032. DOI: 10.1109/LMWC.2020.3025698

[5] XIE, H. W., ZHOU, K., ZHOU, C. X., et al. Compact SIW diplexers and dual-band bandpass filter with wide-stopband performances. *IEEE Transactions on Circuits and Systems. II, Express Briefs*, 2020, vol. 67, no. 12, p. 2933–2937. DOI: 10.1109/TCSII.2020.2992059

[6] DONG, Y. D., YANG, T., ITOH, T. Substrate integrated waveguide loaded by complementary split-ring resonators and its applications to miniaturized waveguide filters. *IEEE Transactions on Microwave Theory and Techniques*, 2009, vol. 57, no. 9, p. 2211–2223. DOI: 10.1109/TMTT.2009.2027156

[7] LI, D., WANG, J., YU, Y., et al. Substrate integrated waveguide-based complementary split-ring resonator and its arrays for compact dual-wideband bandpass filter design. *International Journal of RF and Microwave Computer-Aided Engineering*, 2020, vol. 31, no. 2, p. 1–9. DOI: 10.1002/mmce.22504

[8] NOURI, K., HADDADI, K., BENZAÏM, O., et al. Substrate integrated waveguide (SIW) inductive window band-pass filter based on post-wall irises. *European Physical Journal: Applied Physics*, 2011, vol. 53, no. 3, p. 1–5. DOI: 10.1051/epjap/2010100057

[9] ADABI, A., TAYARANI, M. Substrate integration of dual inductive post waveguide filter. *Progress In Electromagnetics Research B*, 2008, vol. 7, p. 321–329. DOI: 10.2528/PIERB08051002

[10] LIU, Q., ZHOU, D., ZHANG, Y., et al. Substrate integrated waveguide bandpass filters in box-like topology with bypass and direct couplings in diagonal cross-coupling path. *IEEE Transactions on Microwave Theory and Techniques*, 2019, vol. 67, no. 3, p. 1014 to 1022. DOI: 10.1109/TMTT.2018.2889450

[11] LIU, Q., ZHANG, D., TANG, M., et al. A class of box-like bandpass filters with wide stopband based on new dual-mode rectangular SIW cavities. *IEEE Transactions on Microwave Theory and Techniques*, 2021, vol. 69, no. 1, p. 101–110. DOI: 10.1109/TMTT.2020.3037497

[12] LI, R., TANG, X., XIAO, F. Design of substrate integrated waveguide transversal filter with high selectivity. *IEEE Microwave and Wireless Components Letters*, 2010, vol. 20, no. 6, p. 328–330. DOI: 10.1109/LMWC.2010.2047518

[13] LIU, H., CHEN, L., WU, S., et al. A new electric coupling and its applications on millimeter-wave SIW filter with high selectivity and controllable TZs. *AEU - International Journal of Electronics and Communication*, 2024, vol. 173, p. 1–8. DOI: 10.1016/j.aeue.2023.154989

[14] ZHU, F., WU, Y., CHU, P., et al. Single-layer substrate-integrated waveguide inline filters with flexible transmission zeros. *IEEE Microwave and Wireless Components Letters*, 2022, vol. 32, no. 6, p. 495–498. DOI: 10.1109/LMWC.2022.3141994

[15] CHEN, X. P., WU, K. Substrate integrated waveguide cross-coupled filter with negative coupling structure. *IEEE Transactions on Microwave Theory and Techniques*, 2008, vol. 56, no. 1, p. 142–149. DOI: 10.1109/TMTT.2007.912222

[16] HE, Z., YOU, C. J., LENG, S., et al. Compact inline substrate integrated waveguide filter with enhanced selectivity using new nonresonating node. *Electronics Letters*, 2016, vol. 52, no. 21, p. 1778–1780. DOI: 10.1049/el.2016.2712

[17] AMARI, S., ROSENBERG, U. Characteristics of cross (bypass) coupling through higher/lower order modes and their applications in elliptic filter design. *IEEE Transactions on Microwave Theory and Techniques*, 2005, vol. 53, no. 10, p. 3135–3141. DOI: 10.1109/TMTT.2005.855359

[18] KHAN, A. A., MANDAL, M. K. Narrowband substrate integrated waveguide bandpass filter with high selectivity. *IEEE Microwave and Wireless Components Letters*, 2018, vol. 28, no. 5, p. 416 to 418. DOI: 10.1109/LMWC.2018.2820605

[19] LIU, Q., ZHOU, D., LV, D., et al. Ultra-compact highly selective quasi-elliptic filters based on combining dual-mode SIW and coplanar waveguides in a single cavity. *IET Microwaves, Antennas and Propagation*, 2018, vol. 12, no. 3, p. 360–366. DOI: 10.1049/iet-map.2017.0516

[20] RHBANOU, A., BRI, S., SABBANE, M. Analysis of substrate integrated waveguide (SIW) resonator and design of miniaturized SIW bandpass Filter. *International Journal of Electronics and Telecommunications*, 2017, vol. 63, no. 3, p. 255–260. DOI: 10.1515/eletel-2017-0034

[21] SIRCI, S., SANCHEZ-SORIANO, M. A., MARTINEZ, J. D., et al. Advanced filtering solutions in coaxial SIW technology based on singlets, cascaded singlets, and doublets. *IEEE Access*, 2019, vol. 7, p. 29901–29915. DOI: 10.1109/ACCESS.2019.2902956

[22] ZHANG, P. J., LI, M. Q. Cascaded trisection substrate-integrated waveguide filter with high selectivity. *Electronics Letters*, 2014, vol. 50, no. 23, p. 1717–1719. DOI: 10.1049/el.2014.3456

[23] LEE, B., LEE, T.-H., LEE, K., et al. K-band substrate-integrated waveguide resonator filter with suppressed higher-order mode. *IEEE Microwave and Wireless Components Letters*, 2015, vol. 25, no. 6, p. 367–369. DOI: 10.1109/LMWC.2015.2421313

About the Authors …

Mai Van TA received the B.E. degree in Electrical and Electronic Engineering from Bauman Moscow State Technical University, Russia, in 2012, the M.E. degree in Electronic Engineering from Le Quy Don Technical University, Vietnam, in 2018, and the D.E. degree in Electrical and Electronic Engineering from Tokyo Institute of Technology, Japan, in 2023. His research interests include microwave circuits and terahertz technologies based on resonant tunneling diodes and photonic crystals.

Huong Thi Thu TRAN received the B.E. degree in Electrical and Electronic Engineering and the M. E. degree in Electronics Engineering from Le Quy Don Technical University, Ha Noi, Viet Nam in 2009 and 2013, respectively. She received the Ph.D. degree from The University of Electro-Communications, Tokyo, Japan in 2017. Her current research interests are in the area of radio and microwave technologies.

Nguyen Tuan HUNG was born in Nam Dinh, Vietnam, on August 2, 1985. He received the B.S., M.S., and Ph.D. degrees in the Department of Electrical and Electronic Engineering from the National Defense Academy of Japan in 2010, 2012, and 2015, respectively. He is currently a lecturer at the Faculty of Radio Electronics, Le Quy Don Technical University, Vietnam. His research interests include the miniaturization and optimal design of antennas for mobile handset devices, communication and radar systems.

Nguyen Duc TRONG received the B.E. degree in Electronics Engineering from Le Quy Don Technical University, Ha Noi, Viet Nam in 2016. He is currently pursuing the M.E. degree in Le Quy Don Technical University. His research interests are microwave devices based on the substrate integrated waveguide technology.

Nguyen Thuy LINH received the B.E. degree in Electrical and Electronic Engineering and the M. E. degree in Electronics Engineering from Le Quy Don Technical University, Ha Noi, Viet Nam in 2009 and 2013, respectively. She received Ph.D. degree from the University of Electro-Communications in Tokyo, Japan in 2020. Now she works as a lecturer and researcher in Le Quy Don Technical University. Her research interests are RF energy harvesting and wireless power transfer, low power analog IC design, RF and THz analog circuit design.

Kieu Khac PHUONG received the B.E. degree in Electrical and Electronic Engineering and the M.E. degree in Electronic Engineering from Le Quy Don Technical University, Ha Noi, Vietnam in 1996 and 2000, respectively. He received the Ph.D. degree in Moscow Institute of Physics and Technology, Moscow, Russia, in 2007. He is currently a lecturer at Le Quy Don Technical University, Ha Noi, Vietnam. His current research interests are in the area of radio and microwave technologies, communication technologies.

Luong Duy MANH received the B.S. and M.S. degrees in Physics from Vietnam National University (VNU) in 2005 and 2007, respectively, and the D.E. degree in Electronics Engineering from the University of Electro-Communications (UEC), Japan, in March 2016. He worked as a postdoctoral researcher at Osaka University, Japan from April 2016 to June 2017. He is currently head of department at Le Quy Don Technical University, Hanoi, Vietnam. His research interests include development of microwave semiconductor devices and circuits and terahertz (THz) integrated systems for wireless communication applications based on resonant tunneling diodes (RTDs) and photonic crystals.